Synthesis of Pyrrolo[2,3-*c*]isoquinolines *via* the Cycloaddition of Benzyne with Arylideneaminopyrroles: Photophysical and Crystallographic Study

Juan-Carlos Castillo,[†,‡] Alexis Tigreros,[†] Yoann Coquerel,[§] Jean Rodríguez,[§] Mario A. Macías,*[,∥] and Jaime Portilla*[,†]

[†]Bioorganic Compounds Research Group, Department of Chemistry, Universidad de los Andes, Carrera 1 No. 18A-10, Bogotá 111711, Colombia.

[‡]Escuela de Ciencias Químicas, Universidad Pedagógica y Tecnológica de Colombia, Tunja 150003, Colombia.

[§]Aix Marseille Université, CNRS, Centrale Marseille, ISM2, 13397 Marseille, France.

[∥]Department of Chemistry, Universidad de los Andes, Carrera 1 No. 18A-12, Bogotá 111711, Colombia.

*Email: jportill@uniandes.edu.co

SUPPORTING INFORMATION

Content:

1. Overview of reactants, substrates and products numbering

5-Amino-1-(*tert*-butyl)-1*H*-pyrrole-3-carbonitrile (**4**), 2,4-dichlorobenzaldehyde (**5c**), benzaldehyde (**5d**), 4-methoxybenzaldehyde (**5e**), 4-(diphenylamino)benzaldehyde (**5f**), 4-fluorobenzaldehyde (**5g**), and 4-bromobenzaldehyde (**5h**).

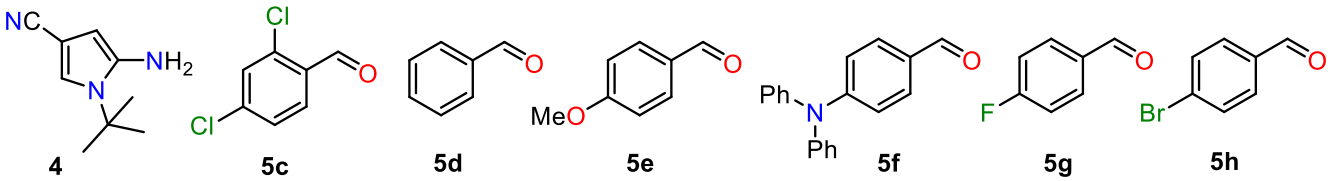

Figure S1. Structure of reactants **4** and **5c–h**

(*E*)-5-(Benzylideneamino)-1-(*tert*-butyl)-1*H*-pyrrole-3-carbonitrile (**6d**), (*E*)-1-(*tert*-butyl)-5-((4-methoxybenzylidene)amino)-1*H*-pyrrole-3-carbonitrile (**6e**), (*E*)-1-(*tert*-butyl)-5-((4-(diphenylamino)benzylidene)amino)-1*H*-pyrrole-3-carbonitrile (**6f**), (*E*)-1-(*tert*-butyl)-5-((4-fluorobenzylidene)amino)-1*H*-pyrrole-3-carbonitrile (**6g**), and (*E*)-5-((4-bromobenzylidene)amino)-1-(*tert*-butyl)-1*H*-pyrrole-3-carbonitrile (**6h**).

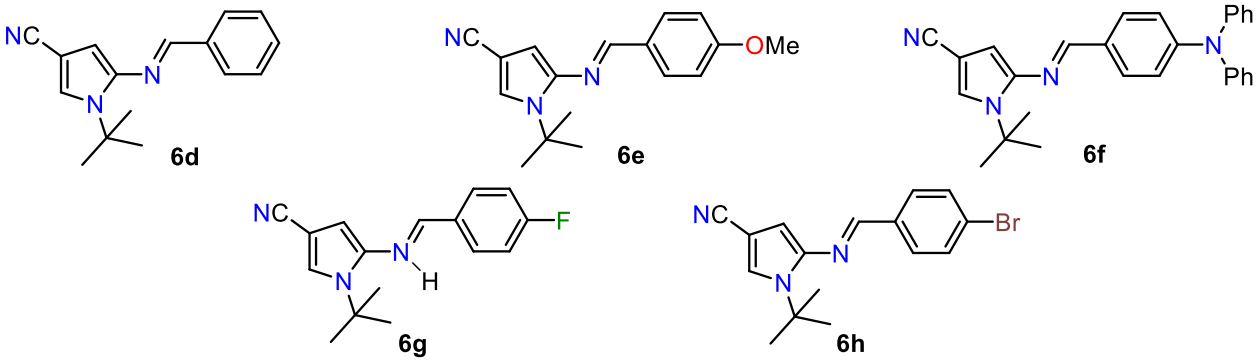

Figure S2. Structure of arylideneaminopyrroles **6d–h**

3-(*tert*-Butyl)-5-(4-methoxyphenyl)-3*H*-pyrrolo[2,3-*c*]isoquinoline-1-carbonitrile (**8a**), 3-(*tert*-butyl)-5-phenyl-3*H*-pyrrolo[2,3-*c*]isoquinoline-1-carbonitrile (**8b**), and 3-(*tert*-butyl)-5-(2,4-dichlorophenyl)-3*H*-pyrrolo[2,3-*c*]isoquinoline-1-carbonitrile (**8c**).

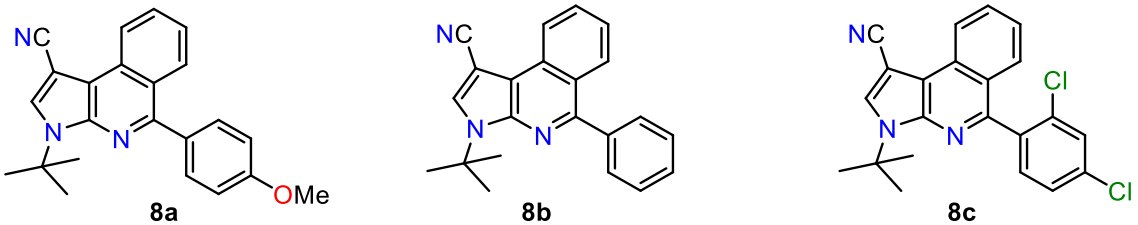

Figure S3. Structure of pyrrolo[2,3-*c*]isoquinolines **8a–c**

2. Copies of NMR spectra of compounds 6d–h and 8a–c

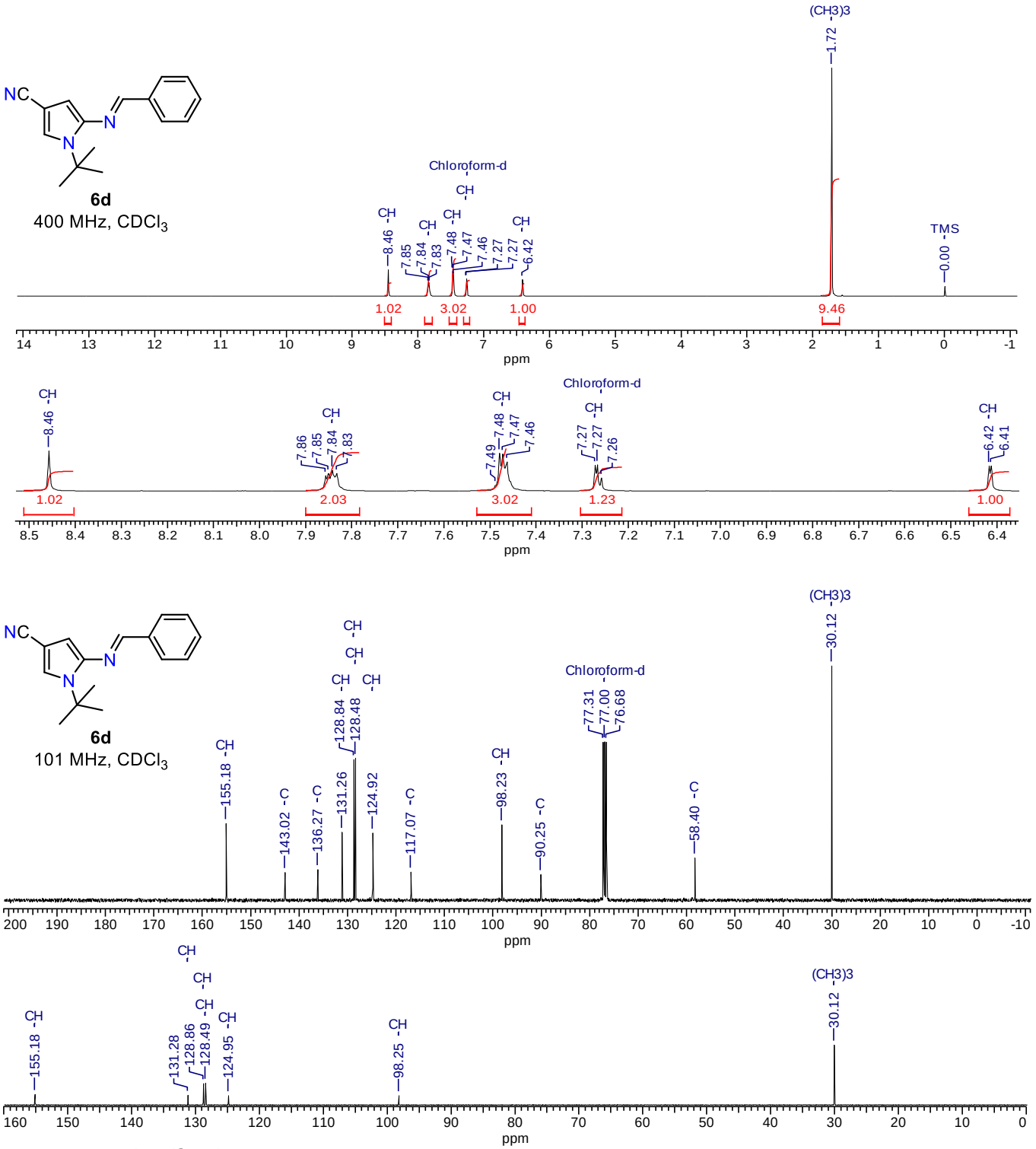

Figure S4. ^{1}H, $^{13}C\{^{1}H\}$, and DEPT-135 NMR spectra of (*E*)-5-(benzylideneamino)-1-(*tert*-butyl)-1*H*-pyrrole-3-carbonitrile **(6d)**

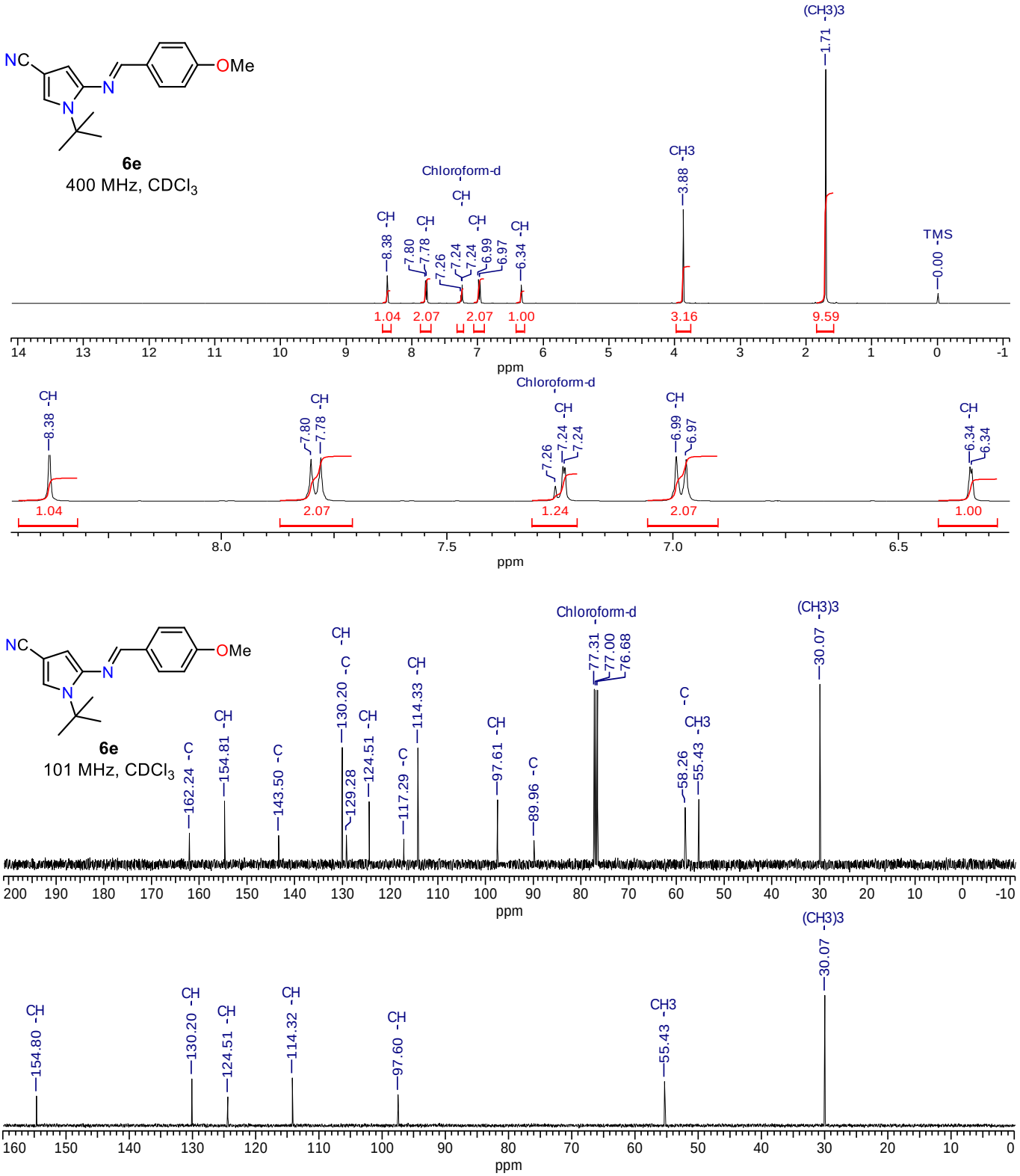

Figure S5. ^{1}H, $^{13}C\{^{1}H\}$, and DEPT-135 NMR spectra of (*E*)-1-(*tert*-butyl)-5-((4-methoxybenzylidene)amino)-1*H*-pyrrole-3-carbonitrile **(6e)**

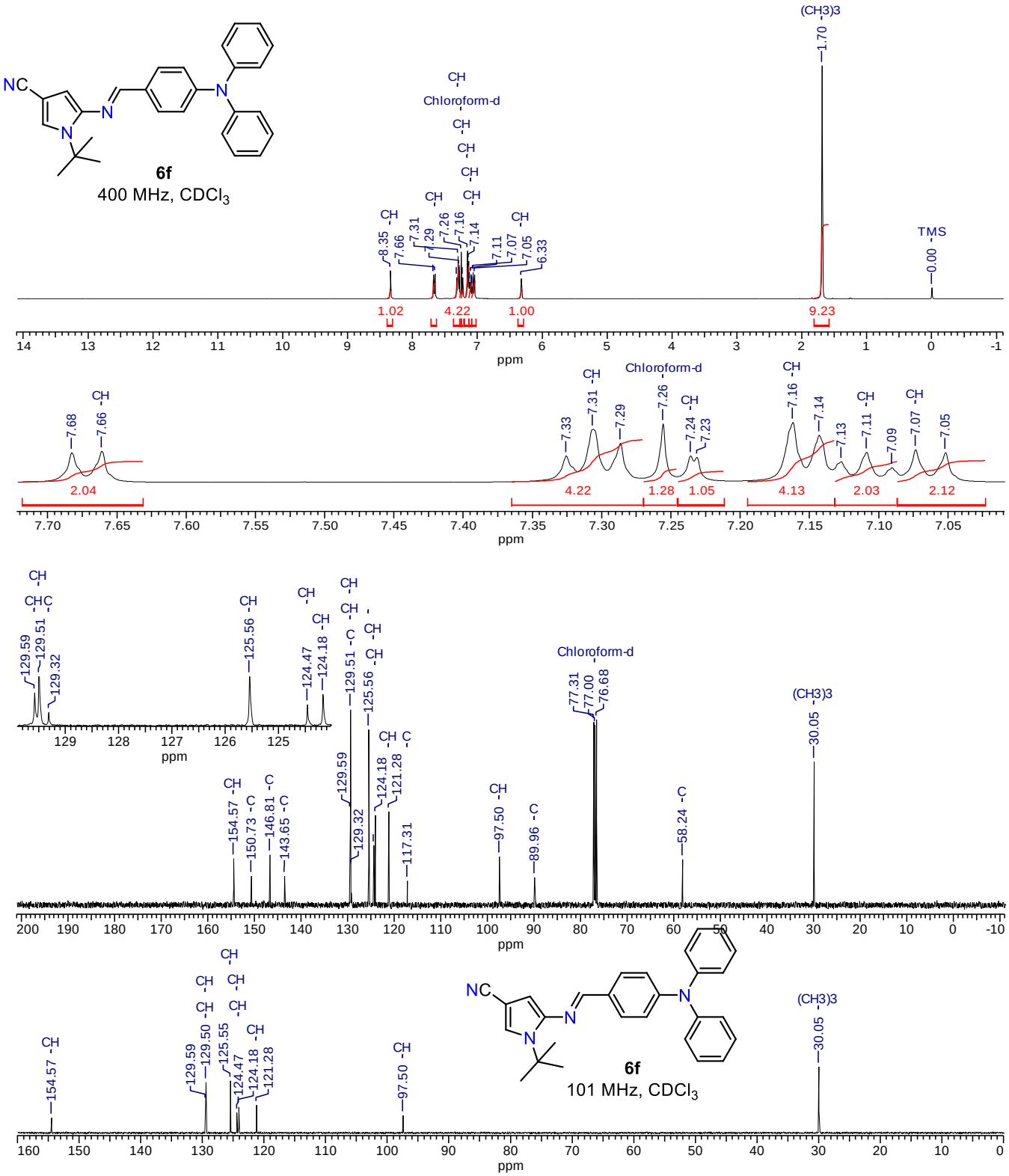

Figure S6. ^{1}H, $^{13}C\{^{1}H\}$, and DEPT-135 NMR spectra of (*E*)-1-(*tert*-butyl)-5-((4-(diphenylamino)benzylidene)amino)-1*H*-pyrrole-3-carbonitrile **(6f)**

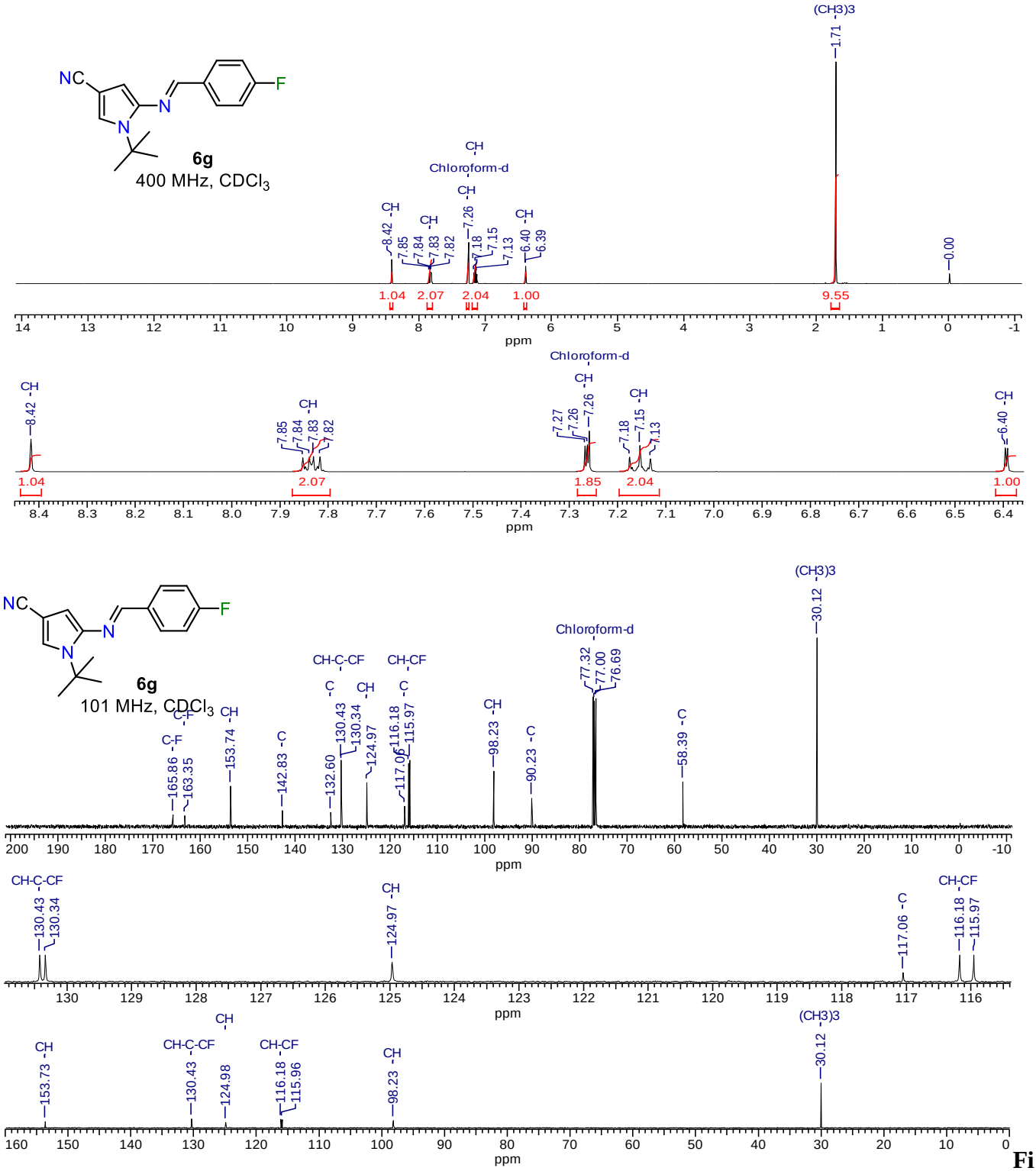

Figure S7. ^{1}H, $^{13}C\{^{1}H\}$, and DEPT-135 of (*E*)-1-(*tert*-butyl)-5-((4-fluorobenzylidene)amino)-1*H*-pyrrole-3-carbonitrile **(6g)**

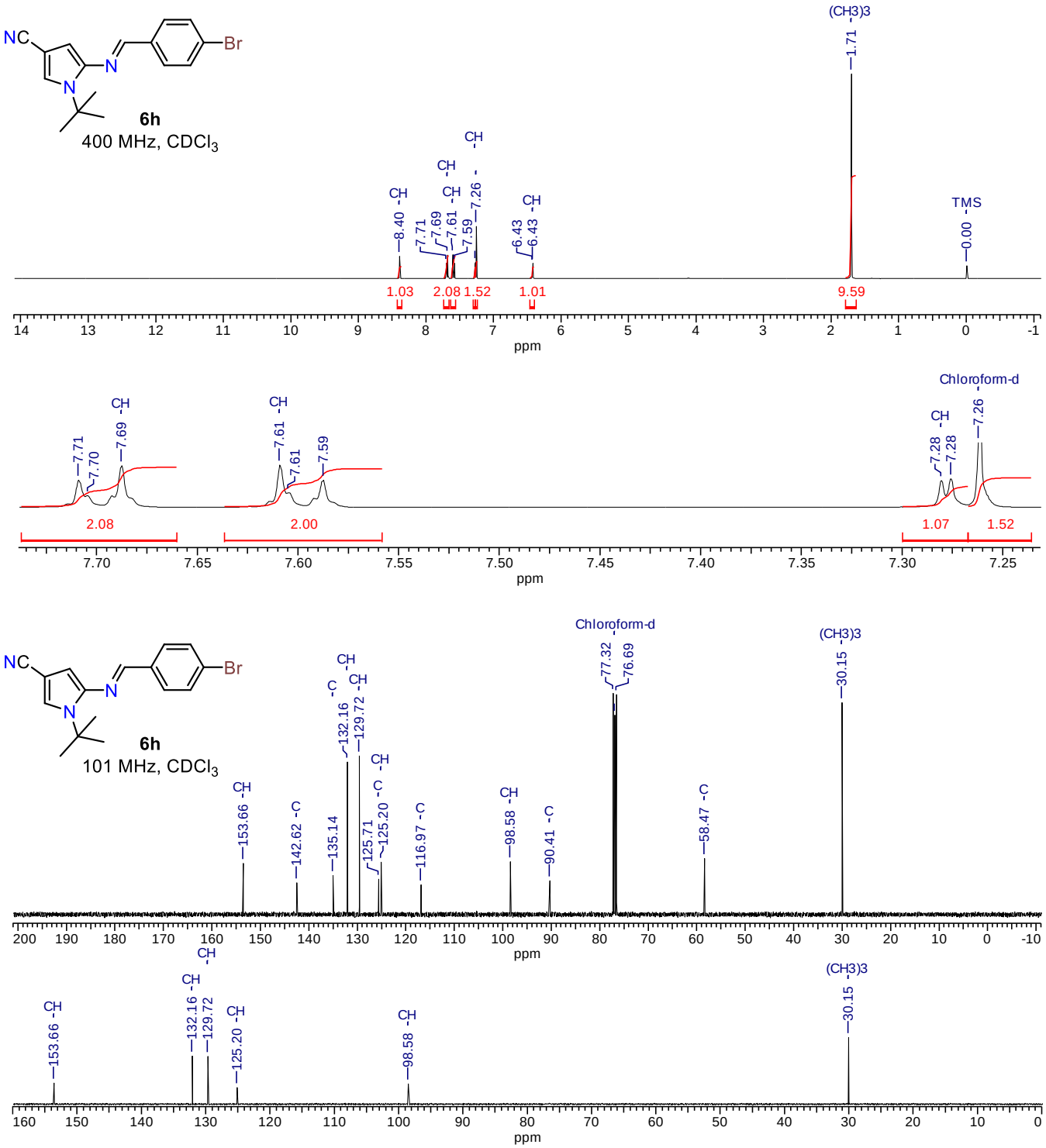

Figure S8. ^{1}H, $^{13}C\{^{1}H\}$, and DEPT-135 of (*E*)-5-((4-bromobenzylidene)amino)-1-(*tert*-butyl)-1*H*-pyrrole-3-carbonitrile **(6h)**

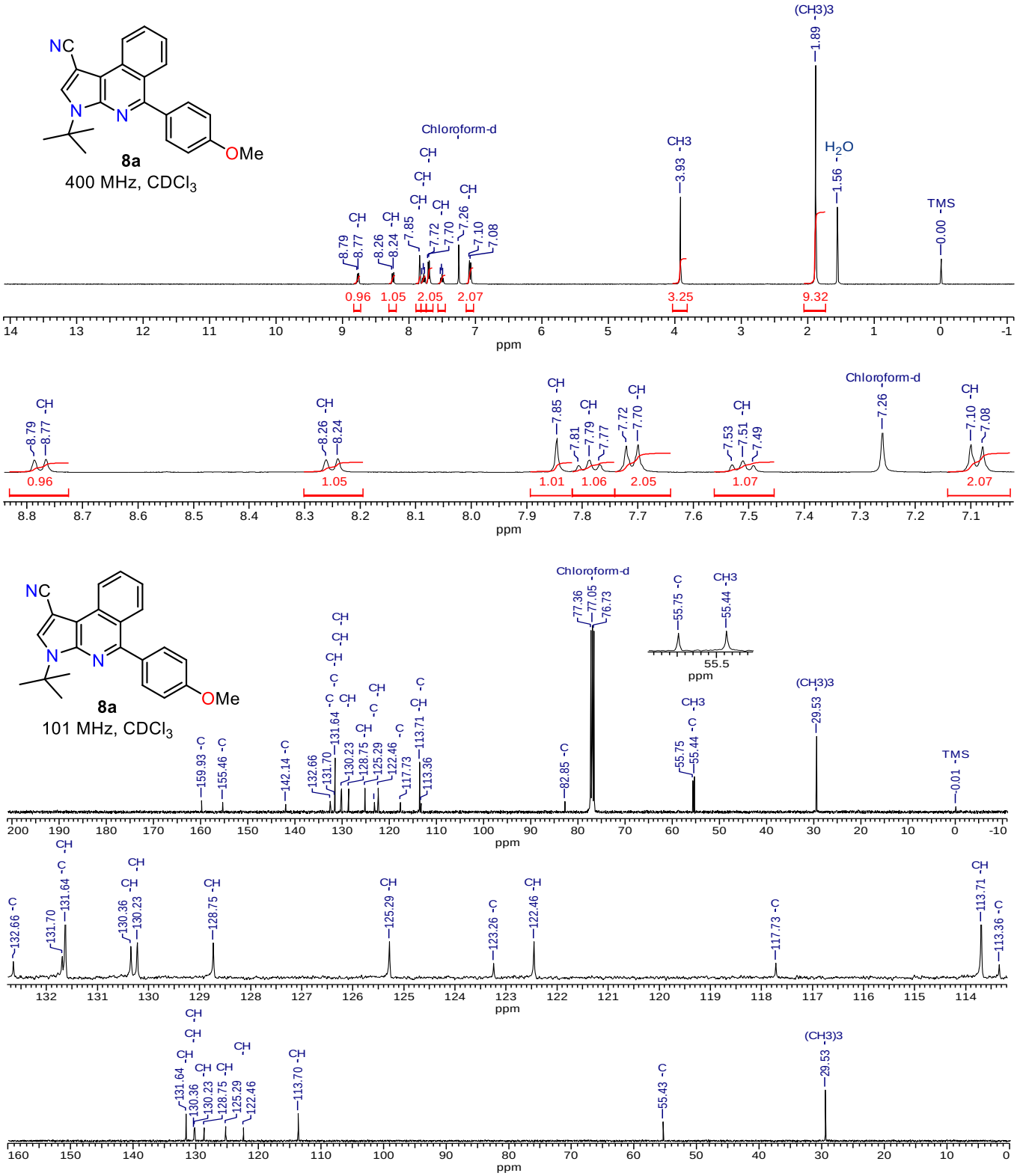

Figure S9. ^{1}H, $^{13}C\{^{1}H\}$, and DEPT-135 NMR spectra of 3-(*tert*-butyl)-5-(4-methoxyphenyl)-3*H*-pyrrolo[2,3-*c*]isoquinoline-1-carbonitrile **(8a)**

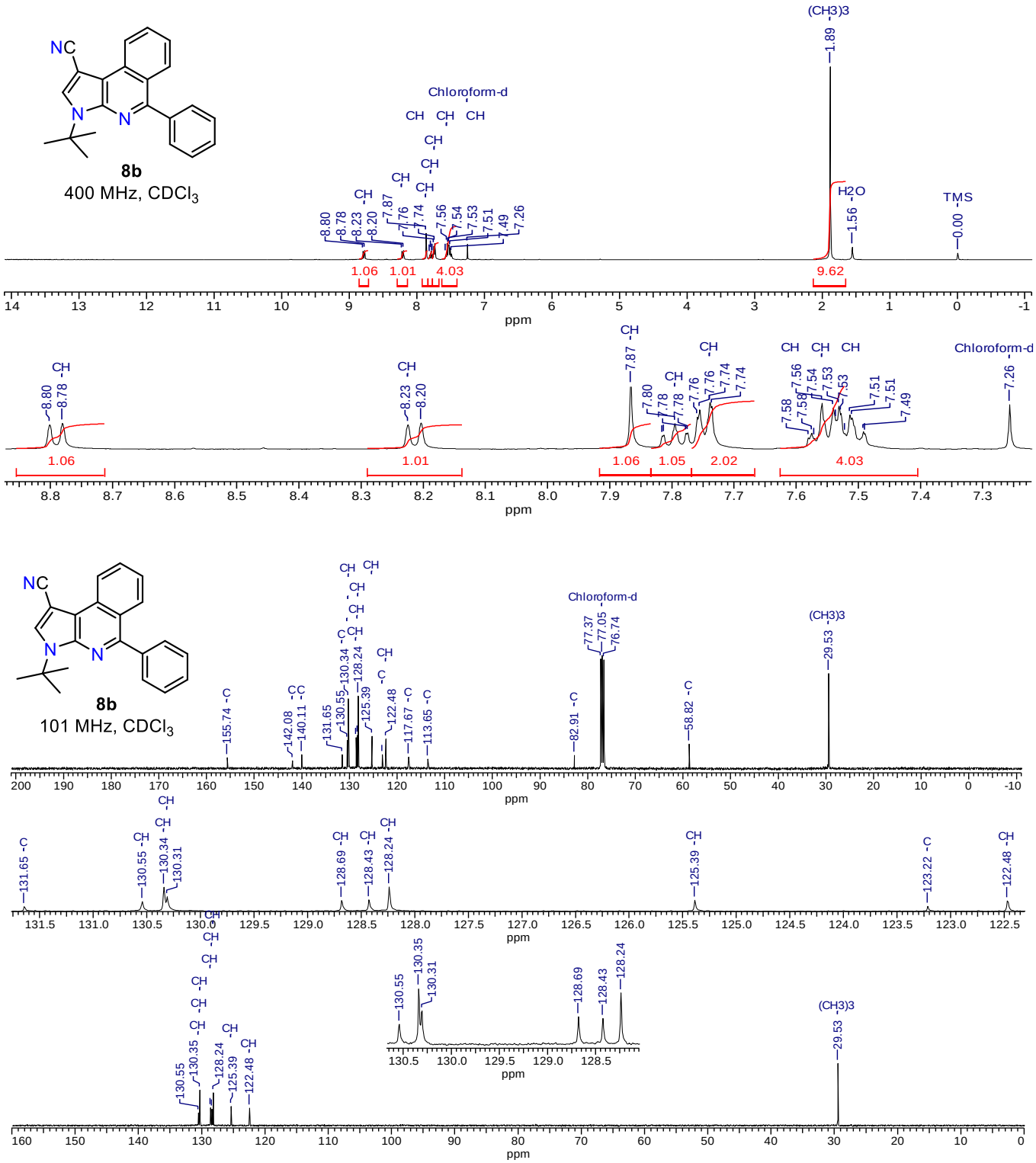

Figure S10. ^{1}H, $^{13}C\{^{1}H\}$, and DEPT-135 NMR spectra of 3-(*tert*-butyl)-5-phenyl)-3*H*-pyrrolo[2,3-*c*]isoquinoline-1-carbonitrile **(8b)**

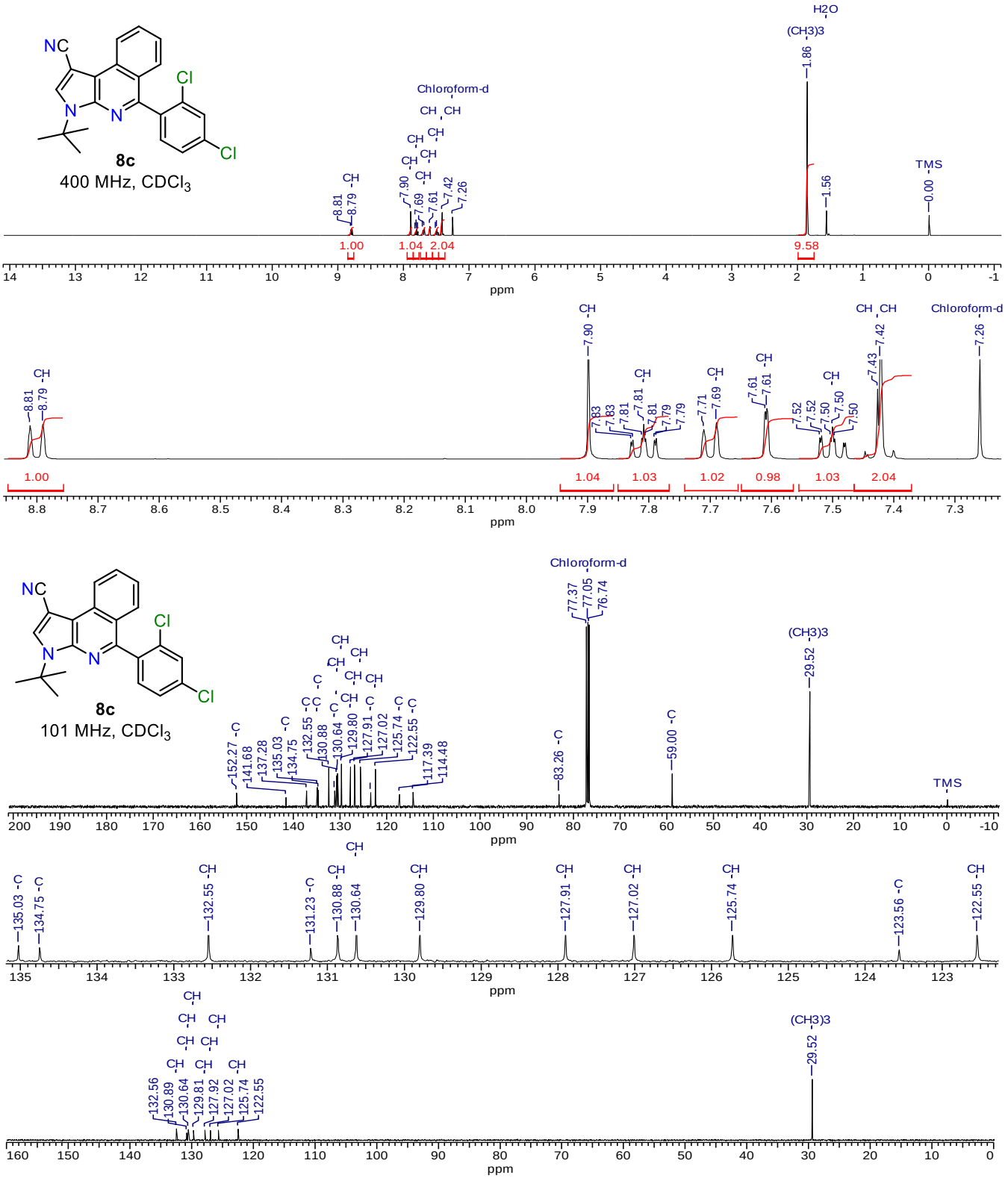

Figure S11. ^{1}H, $^{13}C\{^{1}H\}$, and DEPT-135 NMR spectra of 3-(*tert*-butyl)-5-(2,4-dichlorophenyl)-3*H*-pyrrolo[2,3-*c*]isoquinoline-1-carbonitrile **(8c)**

3. HRMS analysis data of novel compounds

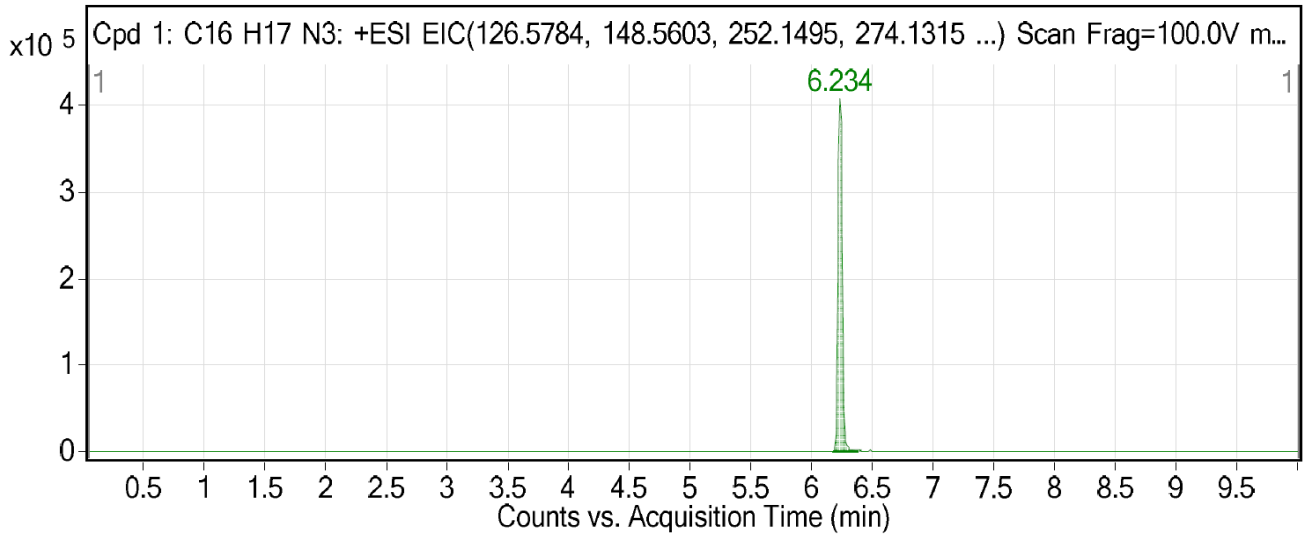

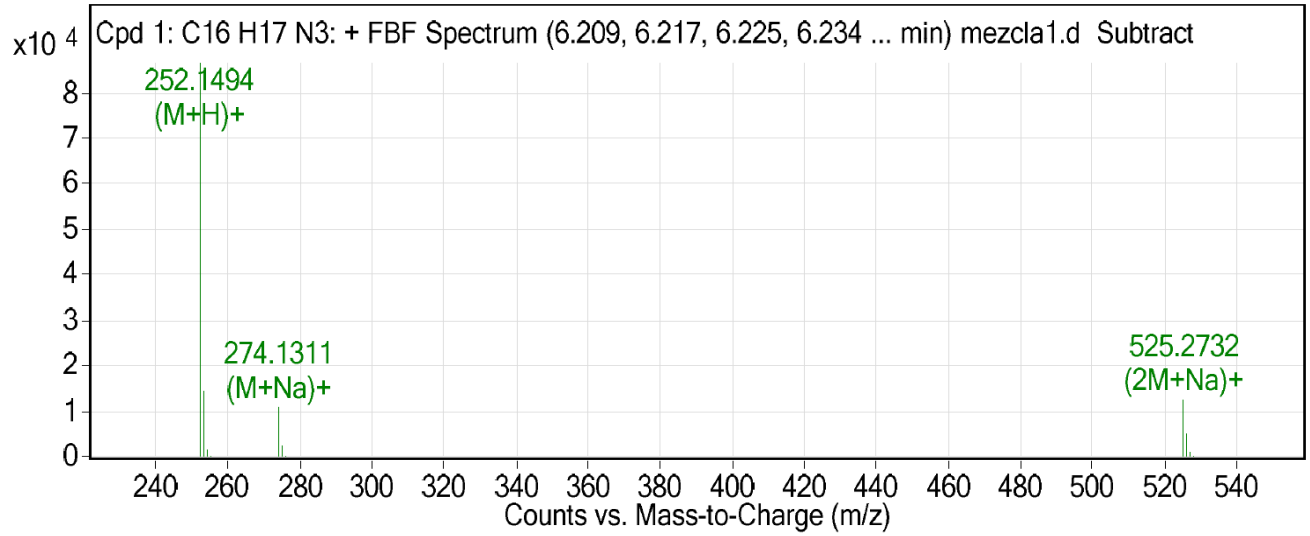

MS Spectrum Peak List

m/z	z	Abund	Ion
252.1494	1	86475.82	(M+H)+
253.1522	1	14186.59	(M+H)+
254.156	1	1271.74	(M+H)+
255.1593	1	183.87	(M+H)+
274.1311	1	10707.49	(M+Na)+
275.1333	1	2276.07	(M+Na)+
276.1378	1	142.61	(M+Na)+
525.2732	1	12417.32	(2M+Na)+
526.2761	1	4937.32	(2M+Na)+
527.2811	1	924.55	(2M+Na)+

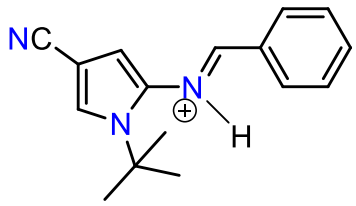

6d + H^+, $C_{16}H_{18}N_3$
Exact Mass: 252.1495
Found: 252.1494

Figure 12. HRMS analysis of compound **6d**

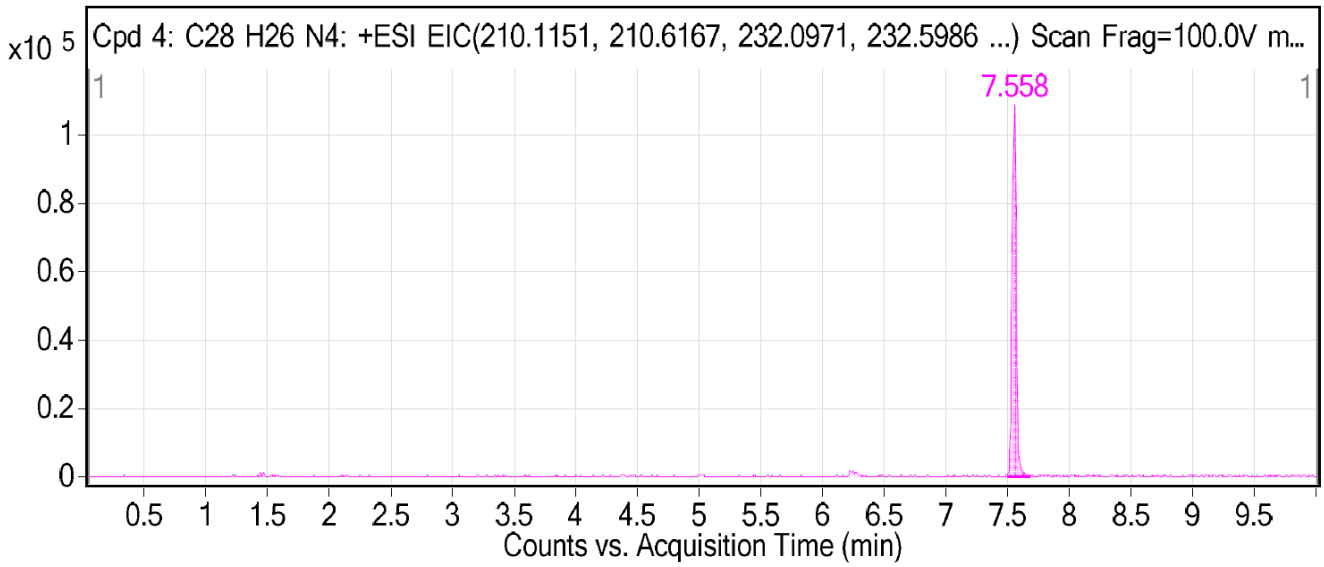

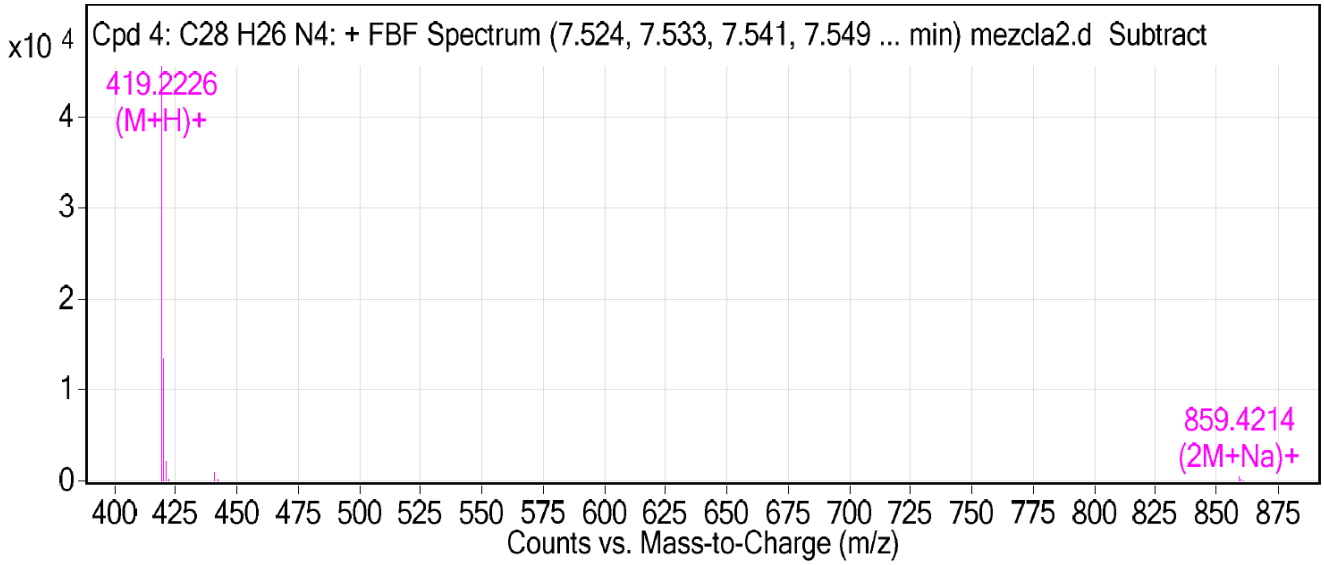

MS Spectrum Peak List

m/z	z	Abund	Ion
419.2226	1	45560.24	(M+H)+
420.2256	1	13501.32	(M+H)+
421.2284	1	2193.37	(M+H)+
422.2323	1	193.97	(M+H)+
441.2033	1	933.88	(M+Na)+
442.2095	1	295.85	(M+Na)+
859.4214	1	462.36	(2M+Na)+
860.4269	1	285.75	(2M+Na)+
861.4331	1	52.68	(2M+Na)+

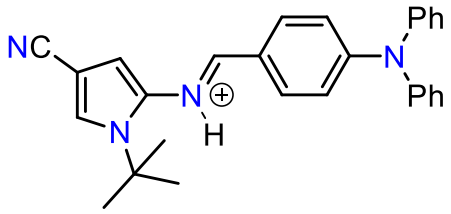

6f + H^+, $C_{28}H_{27}N_4$
Exact Mass: 419.2230
Found: 419.2226

Figure 13. HRMS analysis of compound **6f**

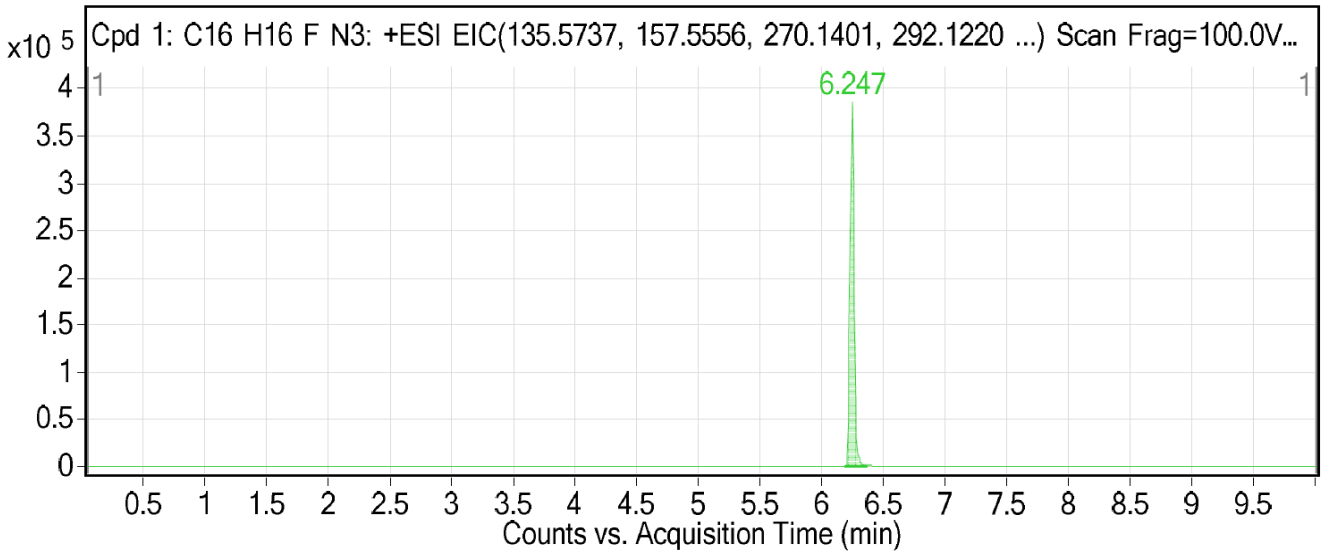

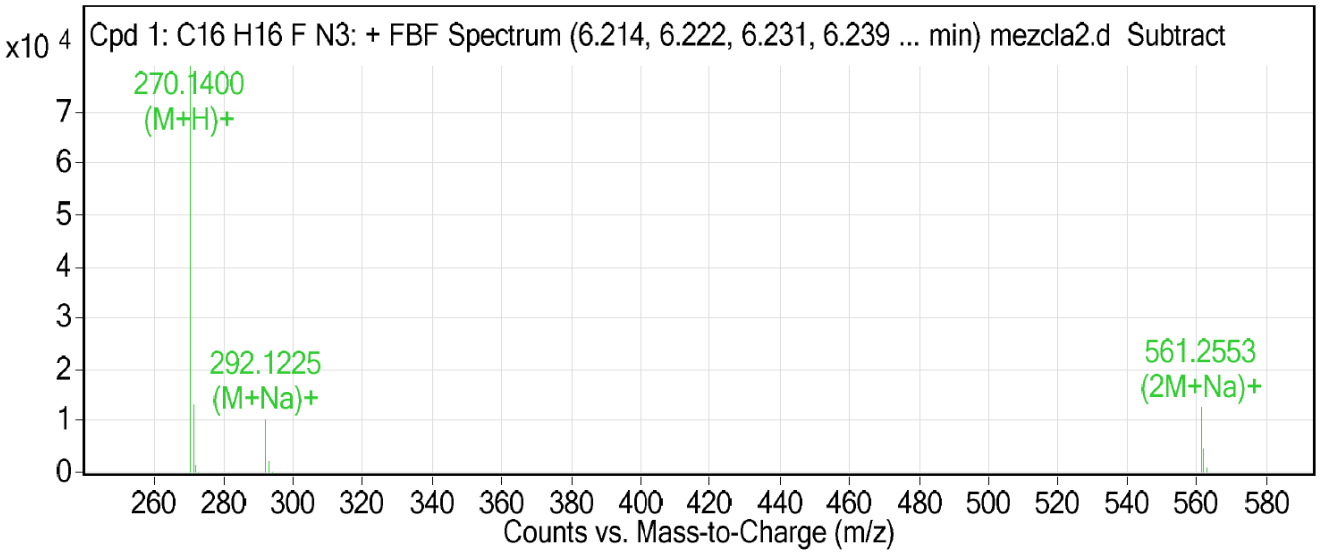

MS Spectrum Peak List

m/z	z	Abund	Ion
270.14	1	78803.33	(M+H)+
271.1434	1	13080.34	(M+H)+
272.1472	1	1242.75	(M+H)+
273.1496	1	130.28	(M+H)+
292.1225	1	10352.38	(M+Na)+
293.1265	1	1856.06	(M+Na)+
294.1272	1	168.23	(M+Na)+
561.2553	1	12609.19	(2M+Na)+
562.2584	1	4610.15	(2M+Na)+
563.2615	1	873.04	(2M+Na)+

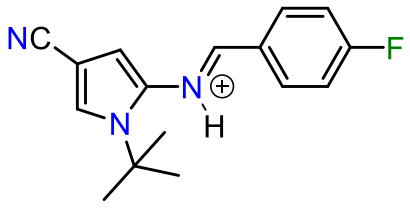

6g + H^+, $C_{16}H_{17}FN_3$
Exact Mass: 270.1401
Found: 270.1400

Figure 14. HRMS analysis of compound **6g**

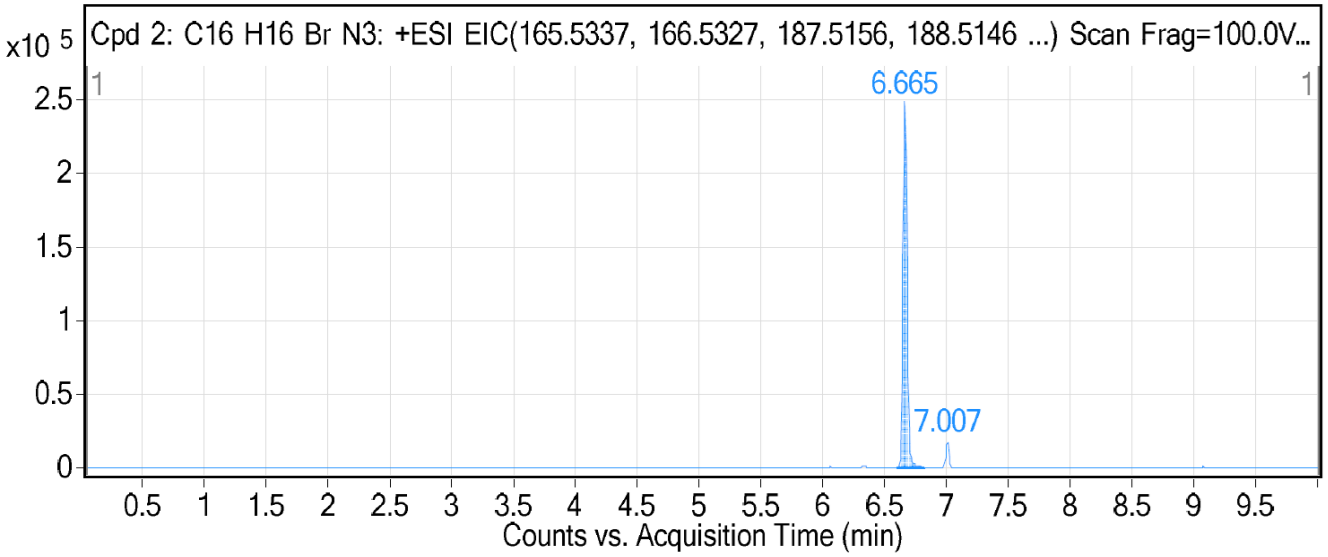

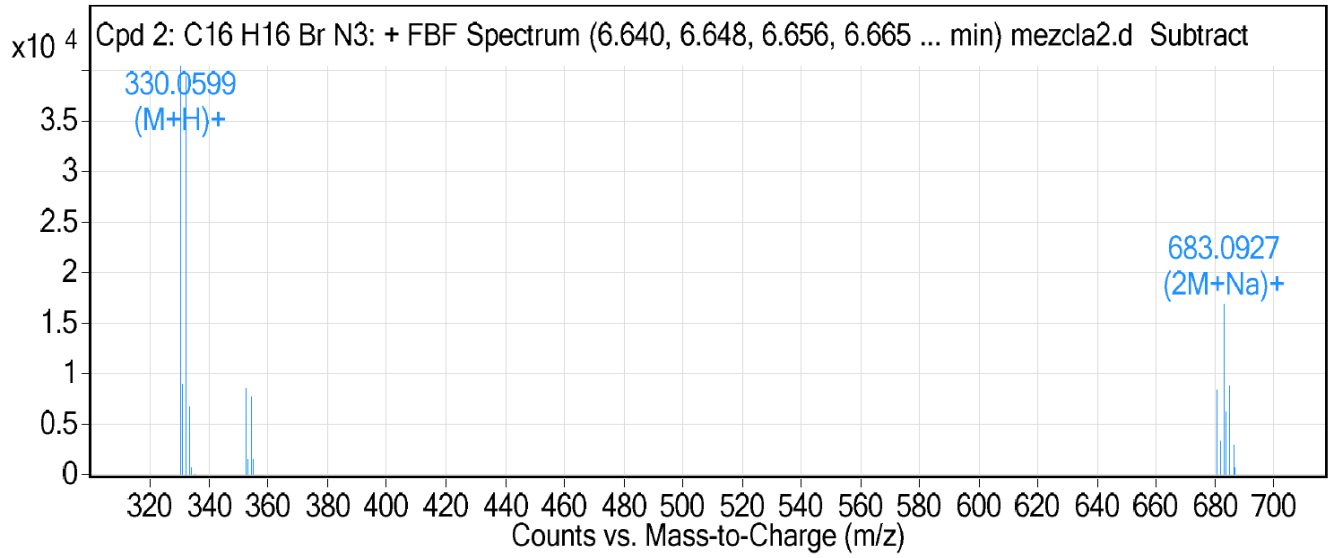

MS Spectrum Peak List

m/z	z	Abund	Ion
330.0599	1	40491.25	(M+H)+
331.0599	1	8915.53	(M+H)+
332.0581	1	39515.48	(M+H)+
333.061	1	6732.12	(M+H)+
352.042	1	8595.27	(M+Na)+
354.0402	1	7679.05	(M+Na)+
681.0944	1	8329.81	(2M+Na)+
683.0927	1	16862.34	(2M+Na)+
684.0953	1	6161.99	(2M+Na)+
685.0911	1	8664.13	(2M+Na)+

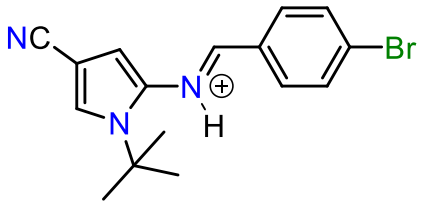

6h + H^+, $C_{16}H_{17}BrN_3$
Exact Mass: 330.0600
Found: 330.0599

Figure 15. HRMS analysis of compound **6h**

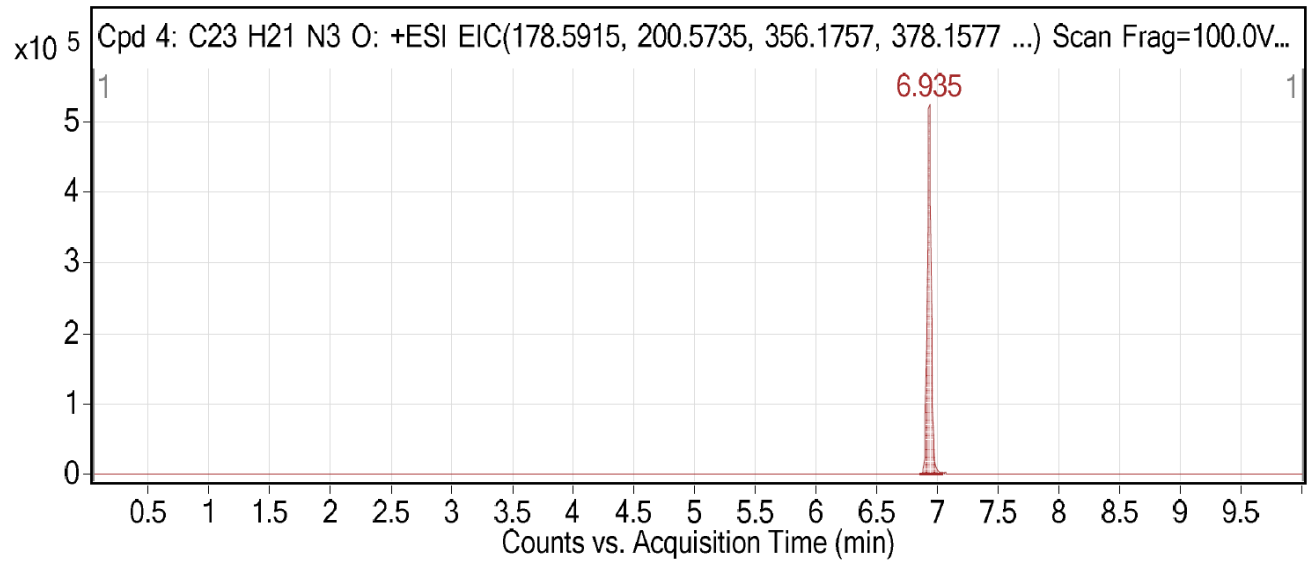

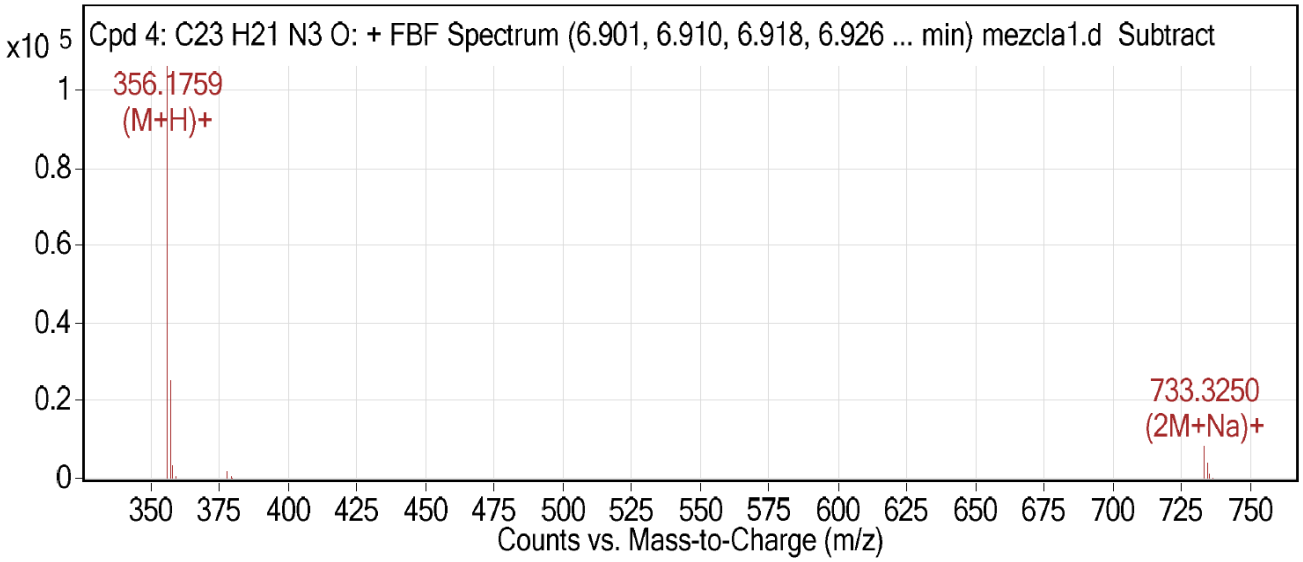

MS Spectrum Peak List

m/z	z	Abund	Ion
356.1759	1	106107.77	(M+H)+
357.1788	1	25264.63	(M+H)+
358.1827	1	3512	(M+H)+
359.1859	1	345.56	(M+H)+
378.1569	1	1903.15	(M+Na)+
379.1589	1	513.67	(M+Na)+
733.325	1	8028.62	(2M+Na)+
734.3282	1	4017.23	(2M+Na)+
735.333	1	1011.23	(2M+Na)+
736.3332	1	167.19	(2M+Na)+

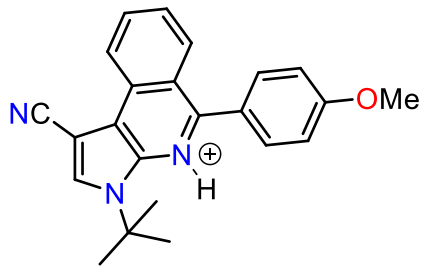

8a + H^+, $C_{23}H_{22}N_3O$
Exact Mass: 356.1757
Found: 356.1759

Figure 16. HRMS analysis of compound **8a**

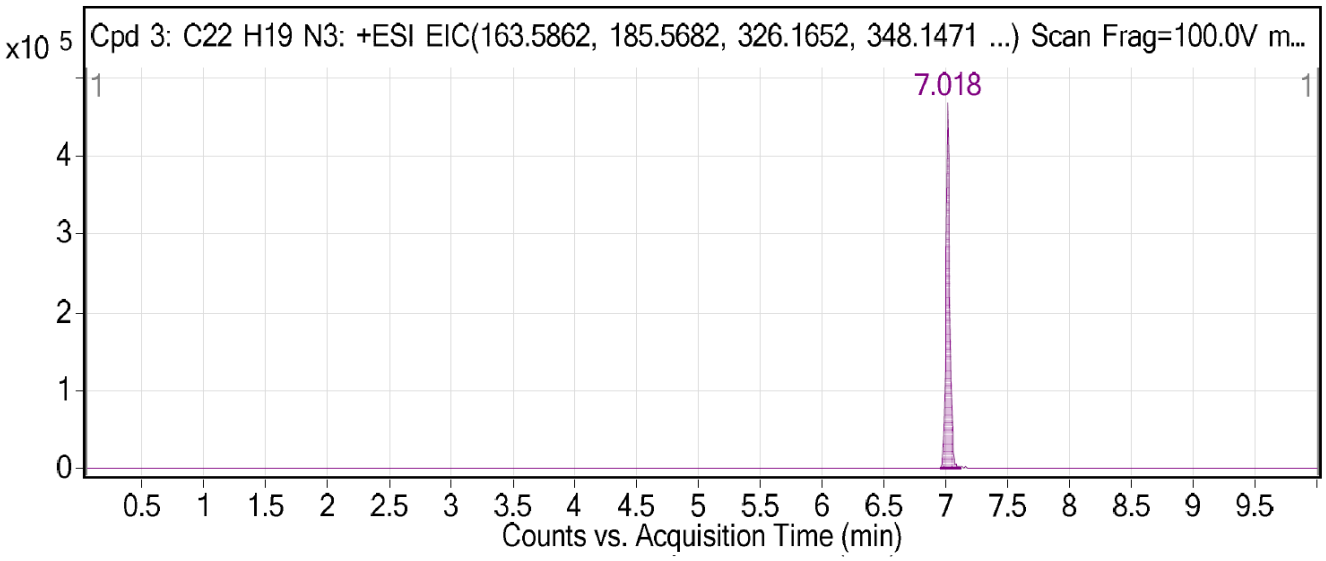

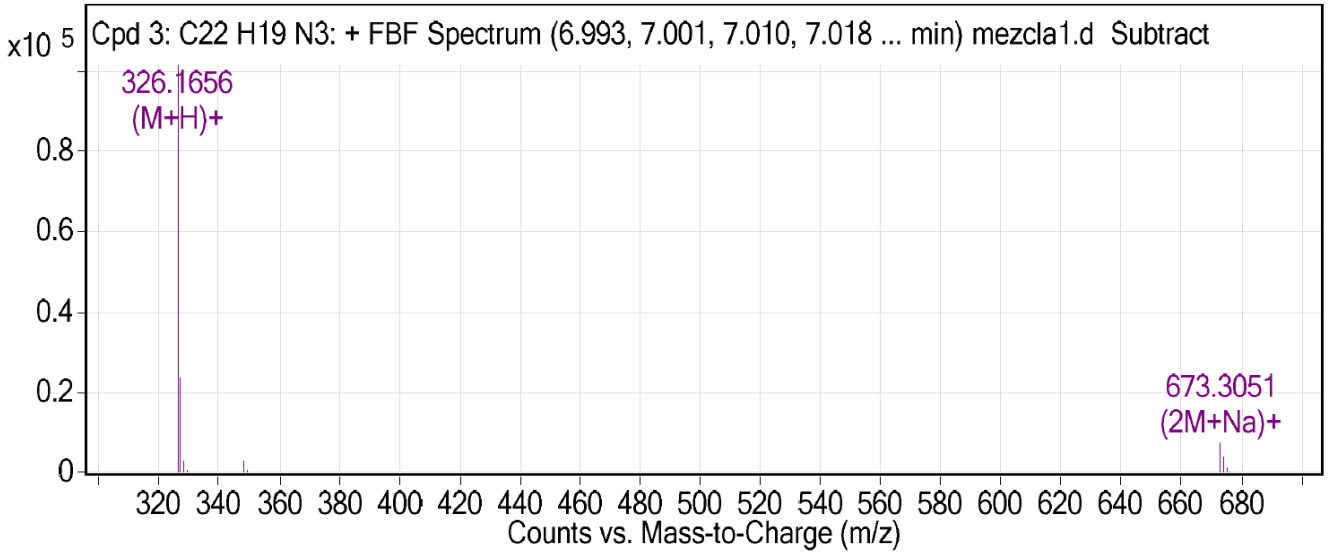

MS Spectrum Peak List

m/z	z	Abund	Ion
326.1656	1	101611.7	(M+H)+
327.1685	1	23636.46	(M+H)+
328.1708	1	2793.57	(M+H)+
329.1729	1	329.5	(M+H)+
348.1482	1	2584.96	(M+Na)+
349.1541	1	524.32	(M+Na)+
673.3051	1	7429.84	(2M+Na)+
674.3085	1	3754.03	(2M+Na)+
675.3104	1	1029.76	(2M+Na)+
676.3115	1	125.03	(2M+Na)+

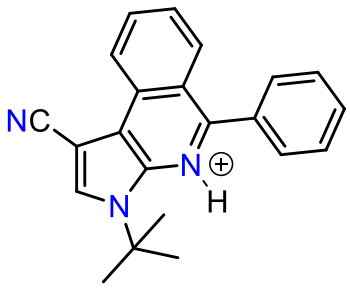

8b + H^+, $C_{22}H_{20}N_3$
Exact Mass: 326.1652
Found: 326.1656

Figure 17. HRMS analysis of compound **8b**

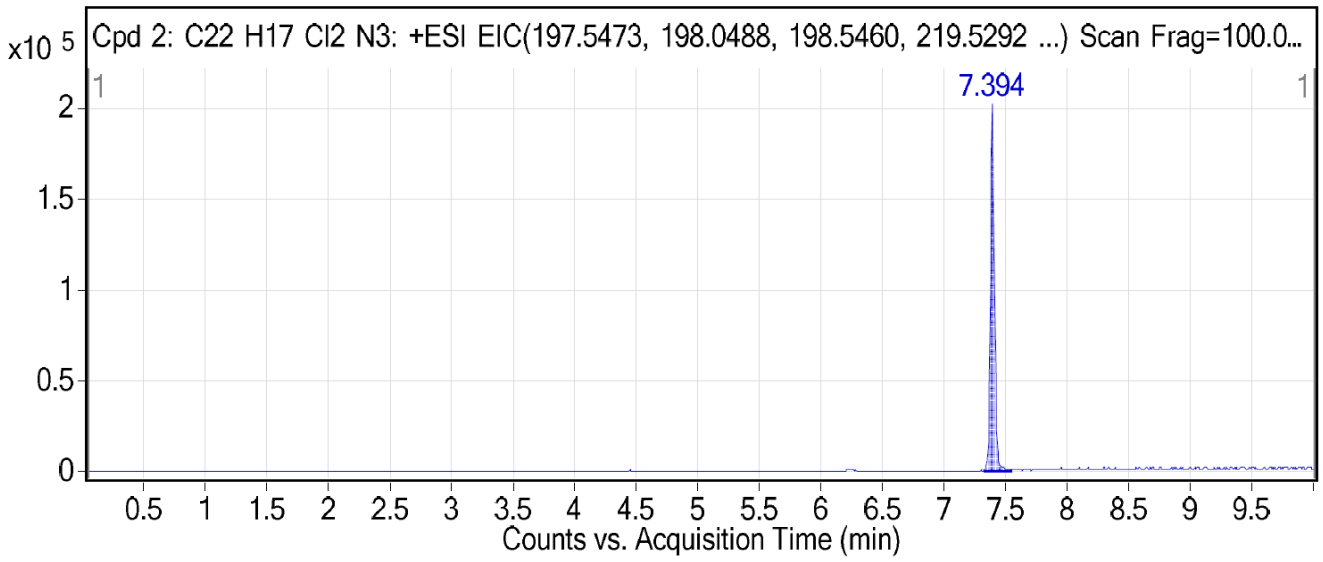

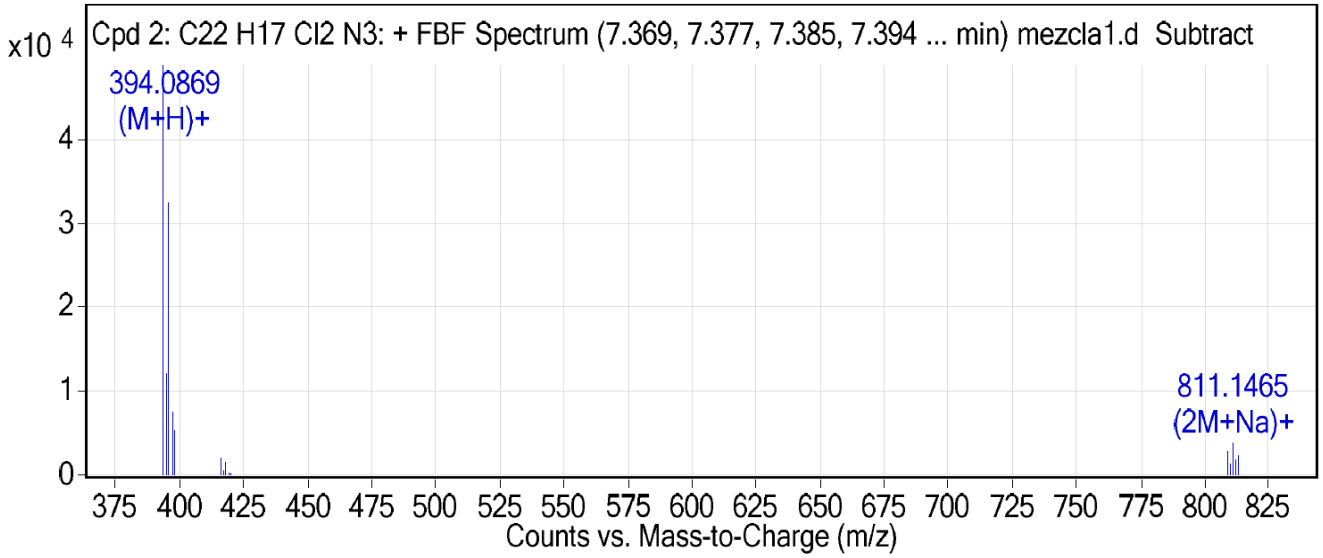

MS Spectrum Peak List

m/z	z	Abund	Ion
394.0869	1	48728.49	(M+H)+
395.0902	1	12029.53	(M+H)+
396.0844	1	32304.44	(M+H)+
397.0873	1	7652.69	(M+H)+
398.0824	1	5307.71	(M+H)+
416.0693	1	2085.37	(M+Na)+
809.1481	1	2794.52	(2M+Na)+
811.1465	1	3879.95	(2M+Na)+
812.1485	1	1723.34	(2M+Na)+
813.1452	1	2198.54	(2M+Na)+

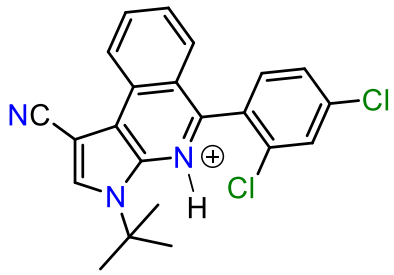

8c + H^+, $C_{22}H_{18}Cl_2N_3$
Exact Mass: 394.0872
Found: 394.0869

Figure 18. HRMS analysis of compound **8c**

4. ORTEP plots of compounds 6e–g and 8b–c

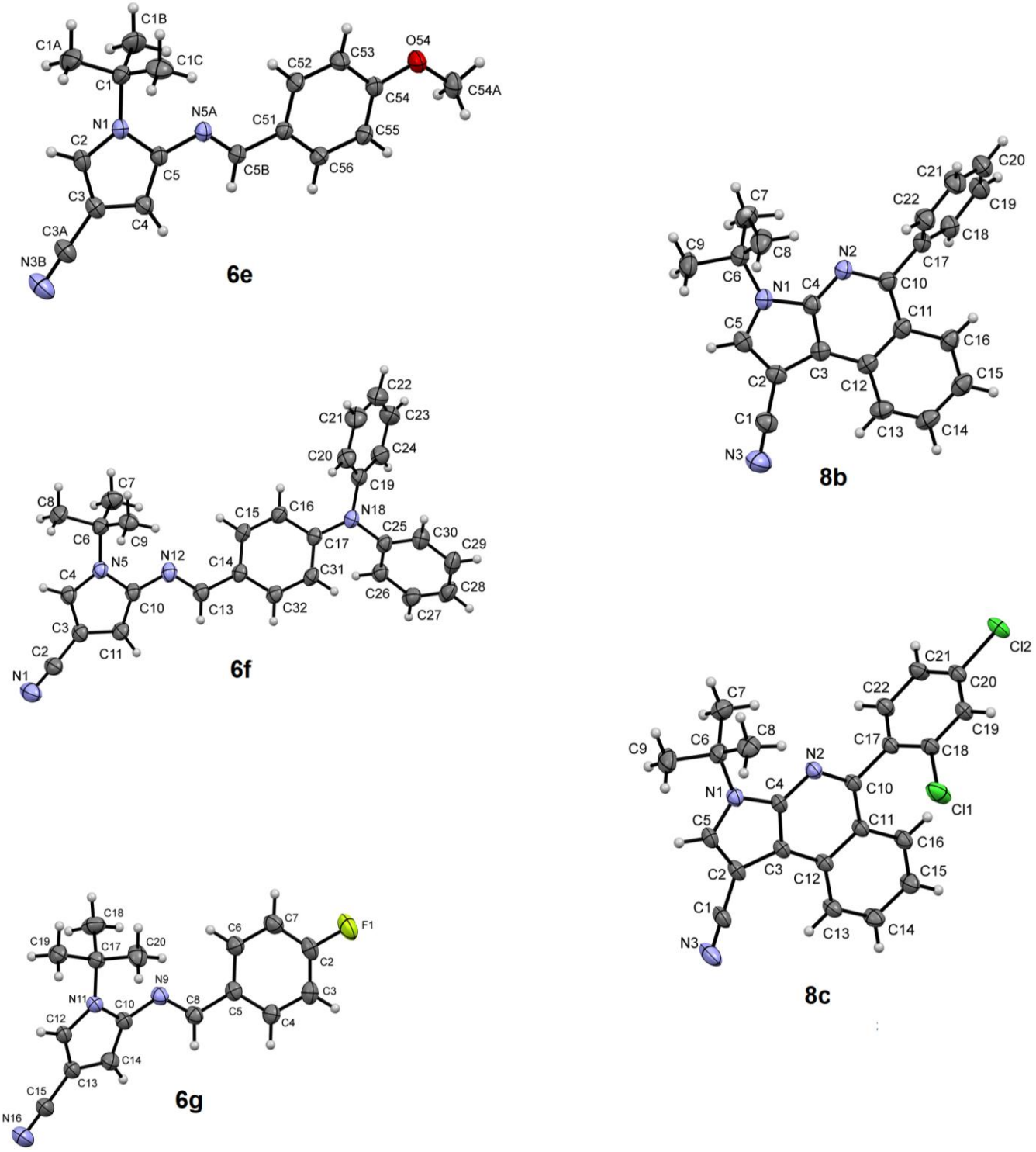

Figure S19. Oak Ridge Thermal Ellipsoid Plots (ORTEP) of the crystal structures showing anisotropic displacement ellipsoids at the 30% probability level. CCDC 1817750 (**6e**), 1817752 (**6f**), 1899534 (**6g**), 1817752 (**8b**), and 1899534 (**8c**), contain the supplementary crystallographic data for this paper.

5. Tables and figures of crystallographic details

Table S1. Crystallographic data for (*E*)-arylideneaminopyrroles **6e–g** and pyrrolo[2,3-*c*]isoquinolines **8b–c**

	6e	**6f**	**6g**	**8b**	**8c**
Crystal data					
Chemical formula	$C_{17}H_{19}N_3O$	$C_{28}H_{26}N_4$	$C_{16}H_{16}FN_3$	$C_{22}H_{19}N_3$	$C_{22}H_{17}Cl_2N_3$
M_r	281.35	418.53	269.32	325.40	394.28
Crystal system, space group	Triclinic, $P\bar{1}$	Monoclinic, $P2_1/c$	Monoclinic, $P2_1/c$	Orthorhombic, $Pna2_1$	Triclinic, $P\bar{1}$
a, b, c (Å)	6.5117(9), 10.8618(15), 12.3586(14)	9.813(2), 25.305(4), 9.7316(11)	8.8167(10), 17.559(2), 9.4619(9)	8.8186(12), 10.9933(15), 18.078(2)	8.4643(7), 9.8411(8), 12.2281(6)
α, β, γ (°)	107.350(11), 96.512(11), 106.366(13)	90.0, 101.981(14), 90.0	90.0, 90.43(1), 90.0	90.0, 90.0, 90.0	97.028(6), 98.958(6), 96.320(7)
V (Å^3)	781.70(19)	2363.9(7)	1464.8(3)	1752.6(4)	989.90(13)
Z	2	4	4	4	2
μ (mm^{-1})	0.08	0.07	0.08	0.07	0.34
Crystal size (mm)	0.31×0.25×0.19	0.23×0.17×0.14	0.21×0.15×0.15	0.21×0.16×0.15	0.25×0.20×0.19
Data collection					
T_{min}, T_{max}	0.804, 1.000	0.849, 1.000	0.801, 1.000	0.575, 1.000	0.681, 1.000
No. of measured, independent and observed [$I > 2\sigma(I)$] reflections	14240, 4319, 3102	24848, 4822, 3145	28818, 2876, 2356	19049, 3840, 3180	43695, 4372, 3475
R_{int}	0.031	0.071	0.067	0.052	0.071
$(\sin\theta/\lambda)_{max}$ (Å^{-1})	0.720	0.626	0.617	0.641	0.641
Refinement					
$R[F^2 > 2\sigma(F^2)]$, $wR(F^2)$, S	0.058, 0.175, 1.10	0.059, 0.177, 1.07	0.057, 0.160, 1.07	0.055, 0.160, 1.11	0.055, 0.156, 1.10
No. of reflections	4319	4822	2876	3840	4372
No. of parameters	195	293	185	230	248
$\Delta\rho_{max}$, $\Delta\rho_{min}$ (e Å^{-3})	0.21, −0.16	0.19, −0.16	0.19, −0.20	0.17, −0.16	0.24, −0.56

Table S2. CE-B3LYP interaction energies (kJ mol^{-1}) for **6e**, **6f** and **6g**[a]

	N	*Symop*	*R*	E_{ele}	E_{pol}	E_{dis}	E_{rep}	E_{tot}	
6e									
	2	x, y, z	6.51	0.1	-3.4	-56.9	24.7	-36.6	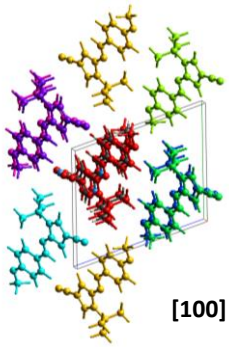 [100]
	2	x, y, z	10.98	1.4	-0.8	-12.5	6.4	-5.9	
	1	-x, -y, -z	13.25	-6.4	-1.0	-17.6	10.2	-16.5	
	1	-x, -y, -z	8.14	-5.9	-1.4	-24.4	14.7	-19.5	
	1	-x, -y, -z	8.88	-5.3	-1.6	-21.1	7.1	-20.8	
	1	-x, -y, -z	6.77	-2.8	-0.4	-22.8	9.0	-17.5	
	1	-x, -y, -z	6.69	-20.6	-6.3	-28.8	22.0	-37.9	
	1	-x, -y, -z	9.07	-19.3	-7.5	-15.2	11.5	-32.1	
6f									
	2	-x, y+1/2, -z+1/2	13.71	-1.2	-0.8	-12.7	3.9	-10.6	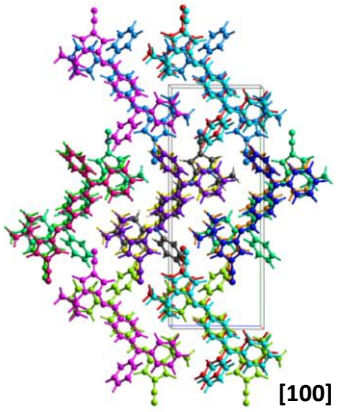 [100]
	1	-x, -y, -z	8.62	-3.4	-0.9	-30.3	11.9	-23.3	
	1	-x, -y, -z	5.39	-9.8	-1.5	-80.4	39.2	-57.3	
	2	x, -y+1/2, z+1/2	13.84	0.1	-0.2	-12.5	2.6	-9.4	
	2	x, y, z	9.73	-2.5	-1.0	-39.9	23.7	-23.5	
	2	-x, y+1/2, -z+1/2	14.24	-5.7	-3.3	-7.4	5.9	-11.3	
	2	x, -y+1/2, z+1/2	13.27	-14.0	-5.1	-18.8	14.6	-26.0	
	1	-x, -y, -z	10.43	-1.8	-0.2	-9.8	2.2	-9.3	
	1	-x, -y, -z	4.89	-11.3	-2.7	-89.5	41.4	-66.3	
	2	-x, y+1/2, -z+1/2	14.58	-5.8	-3.2	-7.4	7.8	-10.1	
6g									
	2	x, y, z	12.88	-6.1	-1.0	-9.0	4.8	-12.1	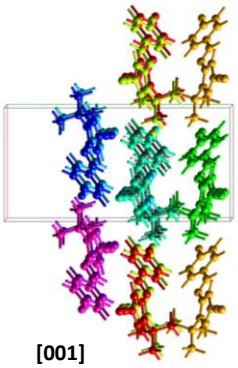 [001]
	2	x, -y+1/2, z+1/2	10.91	-0.6	-0.3	-10.7	3.6	-7.9	
	2	x, y, z	8.82	0.8	-0.7	-16.7	9.3	-8.5	
	2	x, -y+1/2, z+1/2	6.48	-2.9	-1.7	-34.9	17.6	-23.8	
	2	x, y, z	9.46	-2.4	-3.2	-15.0	4.6	-15.1	
	1	-x, -y, -z	5.53	-1.9	-2.3	-54.7	26.0	-35.2	
	1	-x, -y, -z	8.72	-31.0	-9.1	-19.1	23.4	-41.7	
	1	-x, -y, -z	8.04	0.0	-0.2	-5.8	1.2	-4.4	
	1	-x, -y, -z	10.44	-16.7	-5.5	-16.4	13.3	-27.8	

[a] N is the number of molecules with an R molecular centroid-to-centroid distance (Å). Electron density was calculated using B3LYP/6-31G(d,p) model energies. Symop is the symmetry operation. Note: (*) scale factors used to determine E_{tot}: E_{ele} = 1.057; E_{pol} = 0.740; E_{dis} = 0.871; E_{rep} = 0.618.

Table S3. CE-B3LYP interaction energies (kJ mol^{-1}) for **8b** and **8c**[a]

8b

N	*Symop*	*R*	E_{ele}	E_{pol}	E_{dis}	E_{rep}	E_{tot}
2	x+1/2, -y+1/2, z	5.72	-12.8	-5.0	-75.1	35.3	-60.9
2	x+1/2, -y+1/2, z	8.57	-5.5	-1.0	-34.8	23.5	-22.4
2	x, y, z	10.99	-5.0	-1.6	-7.7	1.9	-12.0
2	-x+1/2, y+1/2, z+1/2	10.87	-2.9	-2.3	-12.5	6.6	-11.5
2	-x, -y, z+1/2	9.43	-5.8	-1.4	-30.3	17.5	-22.7
2	x, y, z	8.82	1.5	-0.1	-4.5	0.1	-2.4
2	-x+1/2, y+1/2, z+1/2	10.87	-0.4	-0.4	-10.6	6.0	-6.3

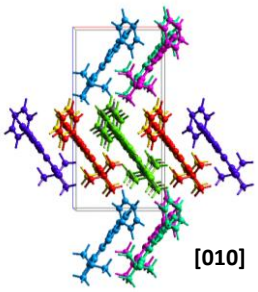

8c

1	-x, -y, -z	7.65	-8.7	-1.9	-50.4	25.4	-38.9
1	-x, -y, -z	13.05	-21.7	-6.5	-13.5	13.8	-31.0
2	x, y, z	12.25	-1.9	-0.5	-11.8	6.4	-8.8
1	-x, -y, -z	11.92	-0.4	-0.2	-3.3	0.1	-3.3
2	x, y, z	8.46	-2.7	-2.1	-36.4	23.9	-21.3
1	-x, -y, -z	10.88	-1.0	-0.1	-6.0	0.8	-5.8
2	x, y, z	9.84	-0.7	-0.1	-6.3	2.2	-5.0
1	-x, -y, -z	7.39	-19.9	-6.7	-72.0	41.7	-62.9
1	-x, -y, -z	11.75	-4.3	-0.4	-14.9	14.6	-8.8
1	-x, -y, -z	7.95	-6.3	-1.6	-46.7	26.9	-31.8
1	-x, -y, -z	8.52	-8.8	-1.3	-42.1	30.6	-27.9

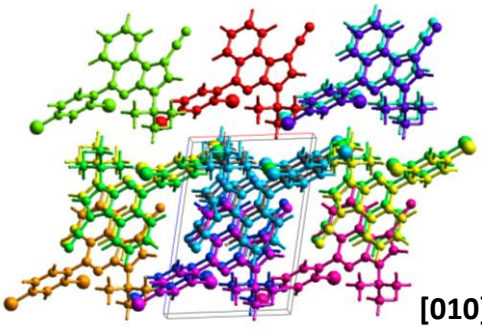

[a] N is the number of molecules with an R molecular centroid-to-centroid distance (Å). Electron density was calculated using B3LYP/6-31G(d,p) model energies. Symop is the symmetry operation. Note: (*) scale factors used to determine E_{tot}: E_{ele} = 1.057; E_{pol} = 0.740; E_{dis} = 0.871; E_{rep} = 0.618.

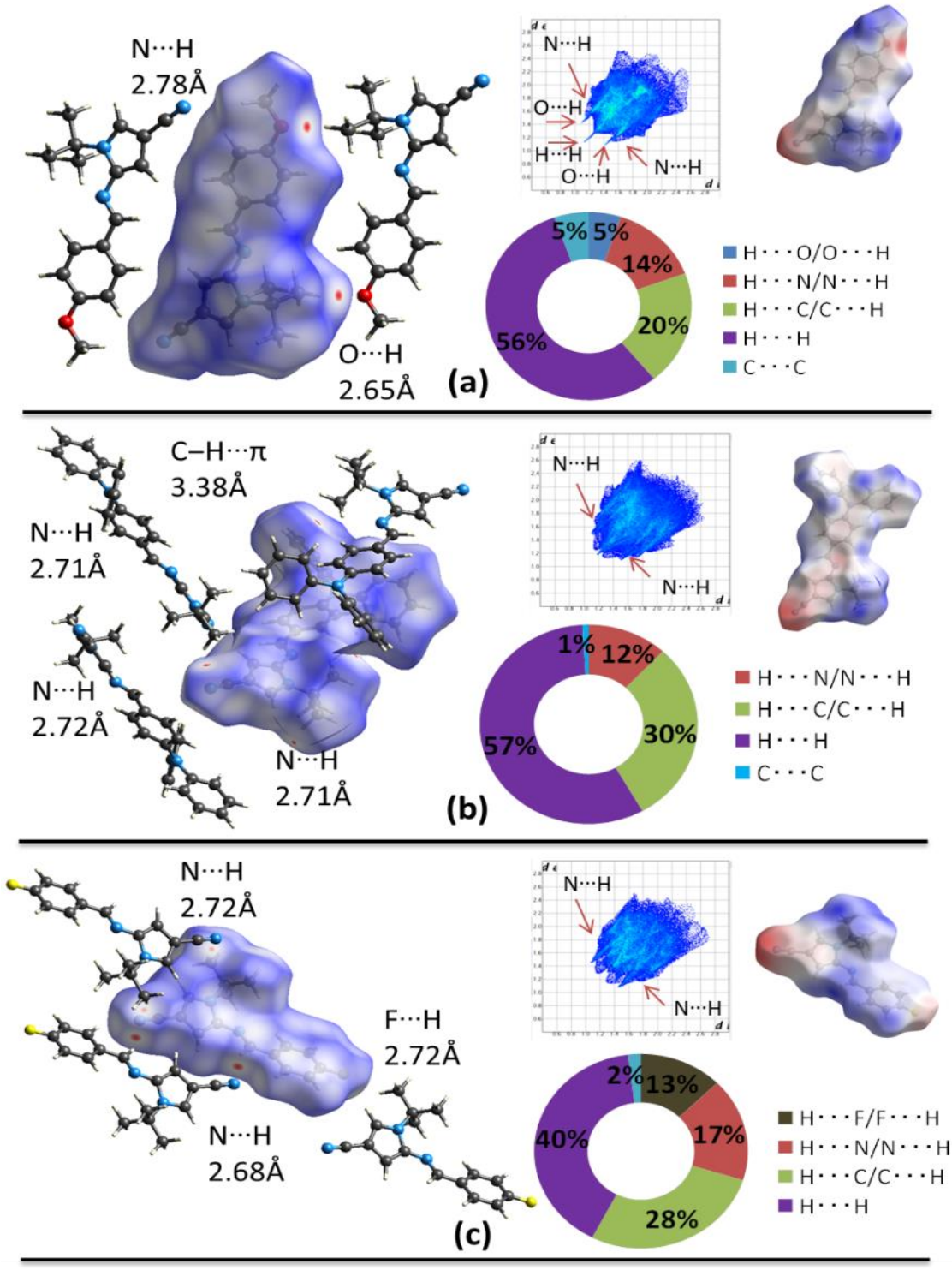

Figure S20. Hirshfeld surfaces mapped over d_{norm}, full 2D fingerprint plots and relative contributions (%) to the Hirshfeld surface area for the various close intermolecular contacts in (a) **6e**, (b) **6f** and (c) **6g**. On the top right-hand corner: the electrostatic potentials with positive and negative potential indicated in blue and red, respectively.

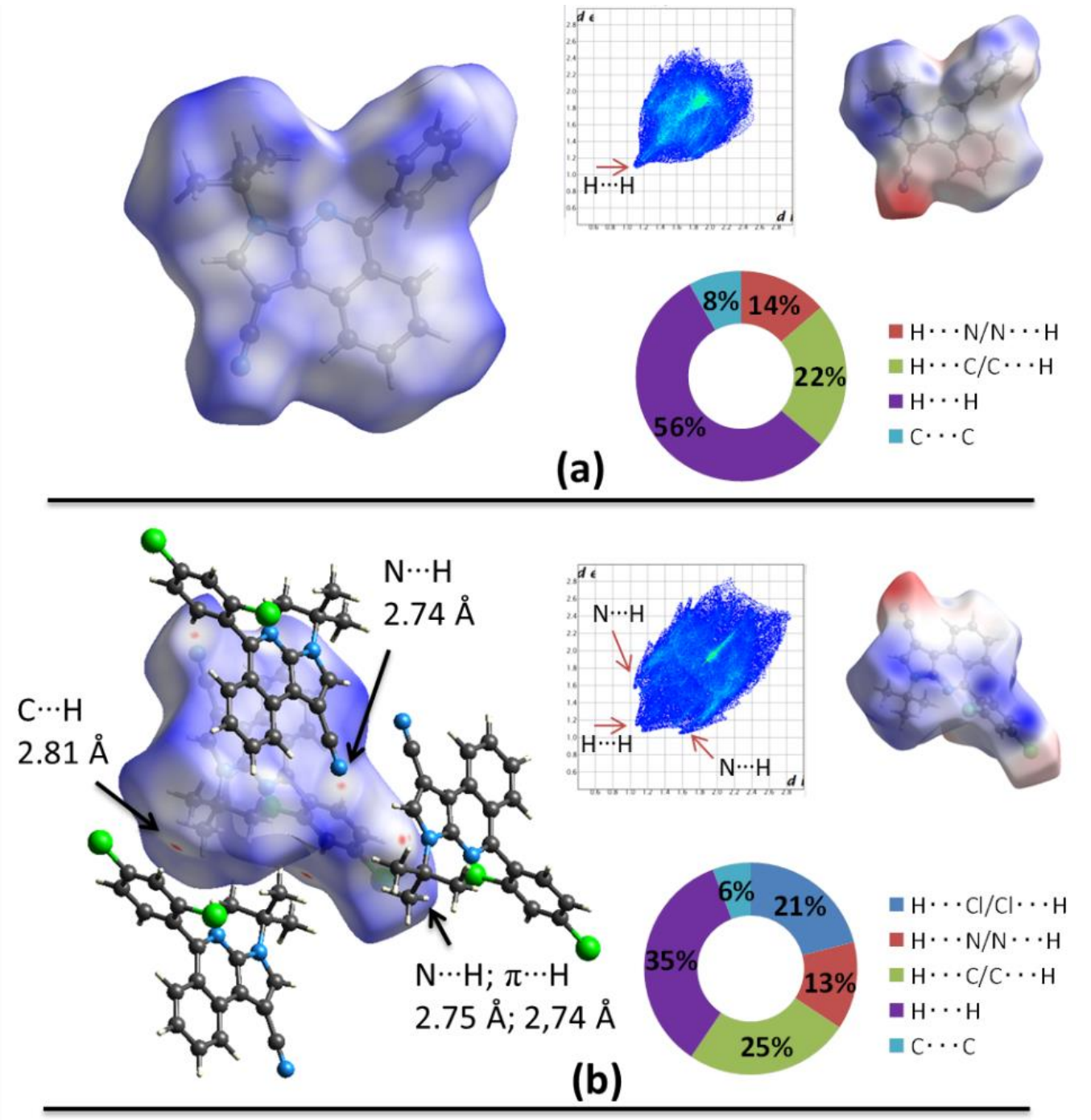

Figure S21. Hirshfeld surfaces mapped over d_{norm}, full 2D fingerprint plots and relative contributions (%) to the Hirshfeld surface area for the various close intermolecular contacts in (a) **8b** and (b) **8c**. On the top right-hand corner: the electrostatic potentials with positive and negative potential indicated in blue and red, respectively.